



This discussion paper is/has been under review for the journal Natural Hazards and Earth System Sciences (NHESS). Please refer to the corresponding final paper in NHESS if available.

# Analysis of synoptic conditions for tornadic days over Western Greece

**P. T. Nastos and I. T. Matsangouras**

Laboratory of Climatology and Atmospheric Environment, Faculty of Geology and Geoenvironment, University of Athens, Panepistimioupolis 15784, Athens, Greece

Received: 27 February 2014 – Accepted: 4 March 2014 – Published: 31 March 2014

Correspondence to: P. T. Nastos (nastos@geol.uoa.gr)

Published by Copernicus Publications on behalf of the European Geosciences Union.

## Analysis of synoptic conditions for tornadic days

P. T. Nastos and  
I. T. Matsangouras

Title Page

Abstract

Introduction

Conclusions

References

Tables

Figures



Back

Close

Full Screen / Esc

Printer-friendly Version

Interactive Discussion





## Analysis of synoptic conditions for tornadic days

P. T. Nastos and  
I. T. Matsangouras

Title Page	
Abstract	Introduction
Conclusions	References
Tables	Figures
⏪	⏩
◀	▶
Back	Close
Full Screen / Esc	
Printer-friendly Version	
Interactive Discussion	

activity worldwide (e.g., Meaden, 1976; Peterson, 1982, 1992, 1995, 1998; Grazulis, 1993; Tarrant, 1995; Tomming et al., 1995; Reynolds, 1999a, b; Tyrrel, 2001; Setvák et al., 2003; Macrinoniene, 2003; Nastos and Matsangouras, 2010; Gayà et al., 2011; Brázdil et al., 2012; Rahuala et al., 2012; Matsangouras et al., 2013). In spite these historical publications, several researchers have presented/analyzed tornadoes occurrences and climatology for many European countries describing the spatio-temporal distribution of these tornadic phenomena (Dessens, 1984; Dessens and Snow, 1987; Paul, 1999; Gayà et al., 2000; Dotzek, 2001, 2003; Holzer, 2001; Bertato et al., 2003; Gianfreda et al., 2005; Giaiotti et al., 2007; Keul et al., 2009; Sioutas, 2011; Matsangouras et al., 2013).

In Greece, significant research has been carried out during the last decade, including tornado and waterspout overviews and climatology (Sioutas, 2003; Nastos and Matsangouras, 2010; Matsangouras et al., 2011a, 2013) and waterspout occurrences and forecasting (Sioutas and Keul, 2007; Keul et al., 2009). In addition to these climatological studies, reports and analyses of some important tornado and waterspout case studies have been performed (Sioutas, 2001, 2002; Sioutas et al., 2006; Matsangouras and Nastos, 2010; Matsangouras et al., 2010, 2011b, 2012; Nastos and Matsangouras, 2012).

The knowledge of spatio-temporal distribution of tornadic events along with the awareness of the synoptic conditions that favour tornadic storms could be characterized as the first stage to set up an effective tornado warning process. This is of high concern in order to help local forecasters to determine the synoptic conditions, which are associated to the development of tornadic events across the different large-scale terrain features of west Greece. Thus, the objective of this study is to compile a 60 year climatology (1953–2012) of tornadoes-waterspouts across west Greece region in order to examine the mean synoptic patterns related to these phenomena, on one hand and on the other hand to interpret the daily composite anomalies of the synoptic conditions with respect to specific isobaric levels. Recognized synoptic weather patterns could be considered by forecasters to detect the potential of tornadic occurrence and





1996), for the period 12 August 1953 to 31 December 2012. The daily composite anomalies of the synoptic conditions were calculated with respect to 30 years climatology (1981–2010).

The analysis of composite means and anomalies of synoptic conditions was carried out in terms of seasonal and monthly variability for specific isobaric levels of 500 hPa, 700 hPa, 850 hPa, 925 hPa and the sea level pressure (SLP). In addition, an analysis and discussion is presented based on the dynamic Lifted index (LI) from NCEP/NCAR Reanalysis datasets.

The analysis of composite means and anomalies of synoptic conditions was carried out with respect to the tornadic type: (a) tornadoes and (b) waterspouts, as it is commonly accepted that different potential processes guide these phenomena. Tornado is known as a rapidly rotating column of air that occurs in association to a cumuli-form cloud. The most intense type of tornado arises within a special type of this cloud, known as a super-cell thunderstorm. Most of what is known in fluid dynamics about tornadoes comes from laboratory and numerical model simulations of the super-cell thunderstorm. It is modelled as a circular updraft fed by air possessing angular momentum with respect to the updraft center axis experiments, simulating vortices that share similarities with what can be observed in a tornado in nature (e.g., Rotunno, 1977, 1978, 1979, 1980, 1984, 2013; Fiedler and Rotunno, 1986; Wilson and Rotunno, 1986; Klemp, 1987; Howells et al., 1988; Fiedler, 2009). Fundamental processes of waterspout formation and detailed structural analyses have been examined by Golden (1973, 1974a, 1974b, 1977), describing the five stages of waterspout: (1) the dark spot, (2) the spiral pattern, (3) the spray ring, (4) the mature waterspout and (5) the decay stage. Golden (1974b) introduced waterspouts association with energy and angular momentum fluxes among five scales of circulation: (1) the funnel scale (3–150 m), (b) the spiral scale (150–1000 m), (c) the individual cumulus-cloud scale (from less than 2 to 10 km), (4) the cumulus cloud-line scale (10–200 km) and (5) the synoptic scale.

**Analysis of synoptic conditions for tornadic days**

P. T. Nastos and  
I. T. Matsangouras

Title Page

Abstract

Introduction

Conclusions

References

Tables

Figures



Back

Close

Full Screen / Esc

Printer-friendly Version

Interactive Discussion







depicts a maximum during November, followed by October, September and December. November is the month with the highest TR frequency, followed by October. Similarly, WS are frequent during November, followed by October, September. This monthly TR distribution over Greece is more different than the respective distribution over central European countries. The maximum monthly TR frequency appears during the warm season (from June to August) over the continental region of central Europe, as already stated by Wegener (1917), Dotzek (2001) and Rahuala et al. (2012).

### 3.2 Synoptic conditions associated to tornado development over west Greece

The synoptic-scale conditions associated to the development of tornadoes, in terms of seasonal and monthly composite analyses, are discussed in this section. Figure 2 shows the daily composite means (left column) and daily composite anomalies (right column) of geopotential heights (m) at 500 hPa isobaric level for TR days during autumn (the most active season), winter, spring and summer. Further, Fig. 3 shows the daily composite means (left column) and daily composite anomalies (right column) of SLP for the aforementioned seasonal periods.

Over the west Greece, the daily composite mean synoptic conditions at 500 hPa level for TR days, during autumn season, are characterized by a broad trough along central and southern Italy, associated with a SW upper-air stream over the study area (Fig. 2). At 700 hPa level (not shown) a long trough is oriented from north Adriatic Sea to Sicily in contrast to the lower pressure levels of 850 hPa and 925 hPa (not shown), where a closed cyclonic circulation is evident over central Italy. The centre of the cyclonic circulation at the surface (1008 hPa) is located over the central Italy and Gulf of Taranto (Fig. 3). The daily composite anomaly of geopotential heights (m) at 500 hPa level appears to be more than  $-120$  m centered over the central Italy (Fig. 2). The maximum composite anomaly (not shown) at 700–850 hPa and 925 hPa lower isobaric levels of the troposphere appears southeasterly, covering a more broad area over south Adriatic Sea, with values equal to  $-90$ ,  $-70$  and  $-50$  m, respectively. Over central Italy, the daily composite anomaly of SLP during TR days is assessed to be  $-8$  hPa (Fig. 3).

## Analysis of synoptic conditions for tornadic days

P. T. Nastos and  
I. T. Matsangouras

Title Page

Abstract

Introduction

Conclusions

References

Tables

Figures



Back

Close

Full Screen / Esc

Printer-friendly Version

Interactive Discussion



Long term means (clino) during autumn season (not shown), based on NCEP/NCAR Reanalysis 1981–2010 period, at 500 hPa and 700 hPa isobaric levels (not shown), revealed a zonal flow over south Europe. At lower isobaric levels (850–925 hPa), a minor trough is located over Corsica (not shown), while a shallow cyclonic circulation is evident over central Mediterranean Sea (Corsica–Italy) against to the eastern Mediterranean Sea, where high geopotential heights over Balkans are combined to a shallow trough over east Mediterranean Sea, establishing an E–SE air flow over west Greece and Ionian Sea.

Daily composite means of synoptic conditions at 500 hPa and 700 hPa isobaric levels (not shown) for TR days during winter season, are characterized by a broad trough along north Italy and over the sea body area between Corsica and southern Italy, associated with a SW upper-air stream over west Greece (Fig. 2). A broad cyclonic circulation is evident from east Corsica to central Adriatic Sea at 700 hPa level (not shown) in contrast to SLP and 925 hPa level (not shown), where the cyclonic circulation is limited over central Italy, causing a SW–S air flow pattern over west Greece. The daily composite anomaly at 500 hPa isobaric level reveals values greater than  $-160$  m over north Italy and a range from  $-40$  m and  $-90$  m over west Greece. The aforementioned maximum anomaly of geopotential heights at 500 hPa level is relocated from NW Italy to central Italy and over the Gulf of Taranto, as we are studying the lower isobaric levels of troposphere (700–850–925 hPa; not shown) and SLP (Fig. 3). Based on NCEP/NCAR long term climatology (not shown) of geopotential heights at 500 hPa and 700 hPa levels, a long trough is located over central Adriatic Sea. At 925 hPa level (not shown) and SLP, a broad shallow low centre appears between Corsica and Italy.

During spring season, the daily composite means reveal a closed cyclonic circulation from middle (500 hPa) to lower isobaric levels of troposphere (Fig. 2). As far as SLP is concerned, the low centre (1009 hPa) is located over central Italy, around the Gulf of Taranto. These synoptic conditions implied a SW air flow over south Ionian Sea and a S–SW air flow pattern over the rest parts of west Greece. Maximum daily composite anomaly at 500 hPa isobaric level ( $-110$  m) appears at the north of Cicely (Fig. 2) and

## Analysis of synoptic conditions for tornadic days

P. T. Nastos and  
I. T. Matsangouras

Title Page

Abstract

Introduction

Conclusions

References

Tables

Figures



Back

Close

Full Screen / Esc

Printer-friendly Version

Interactive Discussion

## Analysis of synoptic conditions for tornadic days

P. T. Nastos and  
I. T. Matsangouras

Title Page

Abstract

Introduction

Conclusions

References

Tables

Figures

⏪

⏩

◀

▶

Back

Close

Full Screen / Esc

Printer-friendly Version

Interactive Discussion

it is relocated smoothly over SE Cicely at lower isobaric levels of 700–850 hPa and 925 hPa (not shown). At SLP, a broad daily composite anomaly is found between Italy and west Greece (Fig. 3). Clino synoptic conditions at 500 hPa and 700 hPa levels (not shown) present a trough line westwards of Italy and a shallow ridge line over south Greece. Regarding the 925 hPa level and the SLP (not shown), the cyclonic circulation is closed between north Cicely and Genoa's Gulf.

Tornadoes during summer days over north parts of Greece are associated to convective weather conditions (unstable atmospheric environment), mainly caused by lower atmospheric heating procedure during summer hot days. Tornadoes over the west parts of Greece are related to the aforementioned heating–instability procedure, but they are also enhanced by a thermo-dynamically unstable environment westwards of Greece. At 500 hPa level, a long trough appears over east Europe tilting to south parts of Italy, causing a west upper air stream (Fig. 2). This trough line at 700 hPa level (not shown) could be described as two separate trough lines; namely, the northern trough line, located along east Europe and the southern trough line along central Adriatic Sea and Corsica. At 850 hPa and 925 hPa isobaric levels (not shown), the northern part of the aforementioned trough line is tilted, causing a meridian air flow pattern. The daily composite mean of SLP reveals a shallow cyclonic circulation over Ionian Sea implying a light S–SW surface air stream over west Greek mainland (Fig. 3). Maximum daily composite anomaly of geopotential heights at 500 hPa during summer days, is identified over central and south parts of Italy with values lower than  $-60$  m and  $-40$  m, over west Greece (Fig. 2). The composite anomalies of geopotential heights over west Greece vary from  $-40$  m to  $-20$  m at lower isobaric levels of 700 hPa, 850 hPa and 925 hPa (not shown). Regarding SLP the anomaly is centred over Taranto's Gulf with values from  $-4$  hPa to  $-3$  hPa (Fig. 3). SLP clino depicts a combination of high pressures over central Europe with low pressure system over Middle East, causing a NE surface air stream. At upper air clino daily composite maps (500 hPa and 700 hPa levels; not shown), a ridge line is evident along Algeria–west Mediterranean Sea, implying a NW upper air stream over west Greece. Studying the isobaric levels of 850 hPa (not

shown), a minor trough is located along north Italy–Corsica, negatively titled and oriented south of Genoa’s Gulf at 925 hPa level (not shown). At both these levels, the upper air stream over the area of interest is from north directions implying a cold dry air mass advection.

5 In the process, the synoptic-scale conditions associated to TR development over west Greece, based on monthly composite analyses, are presented. Daily composite means of SLP (not shown) during cold months (December and January) reveal a closed cyclonic circulation over north Ionian Sea and Taranto’s Gulf, with isobar lines of 1009 hPa and 996 hPa, respectively. S–SW surface air stream is established  
10 over west Greece as a low pressure system appears over Corsica (1005 hPa) during TR days in February. During March and April, a broad closed low pressure system (1011 hPa and 1010 hPa, respectively) is present over Ionian Sea and south Italy, in contrast to a shallow cyclonic circulation over Genova’s Gulf during TR days, in May. During hot season months (June, July and August), a shallow unclosed cyclonic cir-  
15 culation is evident over north Ionian Sea and Taranto’s Gulf, as high pressure system over central Europe is combined to low pressure system over east Mediterranean Sea. During autumn months (September, October and November) a closed cyclonic cir-  
20 culation is identified over central Italy and is relocated further SE to Taranto’s Gulf as we passing from September to November with a steady 1009 hPa pressure centre, implying a surface wind from south directions over north Ionian Sea and S–SW winds over south Ionian Sea and Peloponnese.

As described in Sect. 3.1, TR intra annual variability revealed that during November and October tornadoes are more frequent. During TR days in November, a long wave trough at 500 hPa level is oriented from NE Italy to the north coasts of Africa, imply-  
25 ing a SW upper air stream. This trough line persists also at 700 hPa level in contrast to 850 hPa and 925 hPa, where a closed cyclonic circulation is located over central Italy. Concerning SLP, a low pressure centre appears over central Italy with a mean pressure of 1004 hPa. During TR days in October, at 500 hPa level, a long trough is identified along north Balkans and east coasts of Italy and a second one between

**Analysis of synoptic conditions for tornadic days**

P. T. Nastos and  
I. T. Matsangouras

Title Page

Abstract

Introduction

Conclusions

References

Tables

Figures



Back

Close

Full Screen / Esc

Printer-friendly Version

Interactive Discussion



## Analysis of synoptic conditions for tornadic days

P. T. Nastos and  
I. T. Matsangouras

Title Page

Abstract

Introduction

Conclusions

References

Tables

Figures

⏪

⏩

◀

▶

Back

Close

Full Screen / Esc

Printer-friendly Version

Interactive Discussion

south France and north of Corsica. At 700 hPa level, the trough is along the Gulf of Taranto and east Cicely. Closed cyclonic circulation is observed over central Italy and south Adriatic Sea, indicating a W–SW air flow stream. At SLP, the low pressure centre (1008 hPa) is located over Taranto's Gulf. The daily composite anomaly of geopotential heights at 500 hPa level during November TR days depicts a maximum (–140 m) over central Italy, which is relocated over central Adriatic Sea as we descend to the lower levels of troposphere. On the contrary, in October, the daily composite anomaly appears over south Adriatic Sea and is relocated further SE at lower isobaric levels. Moreover, the anomalies of geopotential heights appearing in October TR days are almost 50 % weaker (–80 m at 500 hPa level) at all barometric levels of lower troposphere, against the respective anomalies appearing in November. The daily composite anomaly of SLP during November is higher over NW Greece, compared to the anomaly of SLP in October.

### 3.3 Synoptic conditions associated to waterspout development over west Greece

Synoptic-scale conditions associated to the development of waterspouts, based on seasonal and monthly composite analyses, are discussed in this section. Figure 4 depicts the daily composite means (left column) and anomalies (right column) of the geopotential heights (m) at 500 hPa for WS days during autumn (the most active season), winter, spring and summer. Besides, Fig. 5 shows the daily composite means (left column) and anomalies (right column) of SLP for the aforementioned seasonal periods.

Over the west Greece, the daily composite mean synoptic conditions at 500 hPa level for autumn WS days, are characterized by a broad trough along central and southern Italy, associated to a SW upper-air stream over west Greece (Fig. 4). At 700 hPa level (not shown), a trough is oriented from north Adriatic Sea to Sicily in contrast to the lower isobaric levels of 850 hPa and 925 hPa (not shown), where a closed cyclonic circulation is identified over central Italy and central Adriatic Sea. Regarding SLP (Fig. 5), a closed cyclonic circulation appears over the central Italy (1011 hPa).



appears to be higher ( $-8$  hPa) over north Greece and Gulf of Taranto, against weaker anomalies within spring ( $-4$  hPa) and summer WS days ( $-2$  hPa) (Fig. 5).

The WS intra annual variability of synoptic conditions (not shown) is discussed further below. The daily composite mean of geopotential heights at 500 hPa level during December WS days reveals a SW air flow over west Greece as a long trough is highlighted along central Adriatic Sea and south parts of Italy. During January and February WS days, the trough line over central Italy maintains the SW upper air flow stream over west Greece. From March to April the upper air stream at 500 hPa level is slightly shifted to westerly flow, as the trough is located over Balkans, against a closed cyclonic circulation over Albania during May WS days. Within June and July WS days, the daily composite mean of geopotential heights at 500 hPa level presents a long trough along eastern parts of Europe and south parts of Italy. The zonal upper air flow within August WS days is shifted towards SW directions during September, October and November, as the trough is established eastwards over Italy. Taking into consideration the surface synoptic conditions, the daily composite mean of SLP, during December to March WS days, depicts a closed cyclonic circulation over the Gulf of Taranto, with the lower value of 1004 hPa in February. The combination of high pressure system over central Europe with low pressure system over eastern Mediterranean Sea implies a shallow cyclonic circulation over Ionian Sea during April, June, July and August. During October and November a closed cyclonic circulation is located over the Gulf of Taranto and central parts of Italy, suggesting a SW surface airflow.

#### 4 Discussion and conclusions

The performed analysis resulted that tornadoes are more frequent over west Greece during autumn season. The daily composite mean of geopotential heights at 500 hPa isobaric level reveals a trough line across north Adriatic Sea and central Italy, associated with a SW upper-air stream over west Greece. During autumn season, the maximum daily composite anomaly of geopotential heights at 500 hPa isobaric level appears

## Analysis of synoptic conditions for tornadic days

P. T. Nastos and  
I. T. Matsangouras

Title Page

Abstract

Introduction

Conclusions

References

Tables

Figures



Back

Close

Full Screen / Esc

Printer-friendly Version

Interactive Discussion





(not shown) over west Greece shows highest median values of  $-21$  hPa during January,  $-12$  hPa during May and  $-10$  hPa during November. Similar findings have been found with respect to the seasonal box and whiskers plots of the daily anomalies of SLP (hPa) for WS days (Fig. 7).

The monthly variability of the dynamic Lifted Index (LI) for TR days is also examined based on NCEP-NCAR reanalysis datasets. Box and whiskers plots of the daily means and anomalies of LI for TR days over west Greece are depicted in Fig. 7 (lower graphs). The median of the daily means of LI (box and whiskers plots) remains below  $-1$  from June to November and thereafter slightly changes with values near to 0 from December to March (Fig. 7, lower left graph). As far as the box and whiskers plots of the daily anomalies of LI are concerned, the median presents the highest negative value in January followed by December, November and October (Fig. 7, lower right graph).

Apart from the analysis of the daily means and anomalies of LI and synoptic conditions at specific isobaric levels, along west Greece, the authors investigated the association of tornado occurrence to frontal waves during the most favourable season (autumn). The association of tornadoes to frontal waves has been considered in recent studies (Clark, 2008; Smart and Browning, 2009; Groenemeijer et al., 2010). Markowski et al. (1998) found that nearly 70% of tornadoes during the Verification of the Origins of Rotation in Tornadoes EXperiment (VORTEX) occurred near a pre-existing baroclinic boundary, most of them within 30 km distance on its cold side.

All examined frontal waves along Ionian Sea, during autumn TR events from 2006 to 2012, based on UK Met Office analysis, have been digitized using Geographical Information System (GIS, ArcGiS). Based on this analysis, the 48% of autumn TR events occur in pre-frontal weather conditions (cold fronts) and 27% appear after the passage of the cold front. Figure 8 illustrates the digitized cold fronts from UK Met Office analysis and TR damage along west Greece, indicating the great impact on the local society, as numerous damage to crops and structures have been recorded (Fig. 8).

*Acknowledgements.* The authors thank the Hellenic National Meteorological Service (HNMS), Hellenic National Library, Aristotle University of Thessaloniki (Psifiothiki), state authorities,

**Analysis of synoptic conditions for tornadic days**

P. T. Nastos and  
I. T. Matsangouras

Title Page

Abstract

Introduction

Conclusions

References

Tables

Figures



Back

Close

Full Screen / Esc

Printer-friendly Version

Interactive Discussion





## Analysis of synoptic conditions for tornadic days

P. T. Nastos and  
I. T. Matsangouras

Title Page	
Abstract	Introduction
Conclusions	References
Tables	Figures
◀	▶
◀	▶
Back	Close
Full Screen / Esc	
Printer-friendly Version	
Interactive Discussion	

Golden, J.: The life-cycle of Florida Keys' waterspouts I, *J. Appl. Meteorol.*, 13, 676–692, 1974a.

Golden, J.: Scale-interaction implications for the waterspout life cycle II, *J. Appl. Meteorol.*, 13, 693–709, 1974b.

5 Golden, J.: An assessment of waterspout frequencies along the US East and Gulf Coasts, *J. Appl. Meteorol.*, 16, 231–236, 1977.

Grazulis, T. P.: Significant Tornadoes, 1680–1991, Environmental Films, St. Johnsbury, VT, 1326 pp., 1993.

10 Groenemeijer, P., Corsmeier, U., and Kottmeier, C.: The development of tornadic storms on the cold side of a front favoured by local enhancement of moisture and CAPE, *Atmos. Res.*, 83, 765–781, 2010.

Holzer, A. M.: Tornado climatology of Austria, *Atmos. Res.*, 56, 203–211, 2001.

Howells, P. A., Rotunno, R., and Smith, R. K.: A comparative study of atmospheric and laboratory-analogue numerical tornado-vortex models, *Q. J. Roy. Meteor. Soc.*, 114, 801–822, 1988.

15 Kalnay, E., Kanamitsu, M., Kistler, R., Collins, W., Deaven, D., Gandin, L., Iredell, M., Saha, S., White, G., Woollen, J., Zhu, Y., Chelliah, M., Ebisuzaki, W., Higgins, W., Janowiak, J., Mo, K.C., Ropelewski, C., Wang, J., Leetmaa, A., Reynolds, R., Jenne, R., and Joseph, D.: The NCEP/NCAR Reanalysis 40-year Project. *B. Am. Meteorol. Soc.*, 77, 437–471, 1996.

20 Keul, A. G., Sioutas, M. V., and Szilagyi, W.: Prognosis of central-eastern Mediterranean waterspouts, *Atmos. Res.*, 93, 426–436, 2009.

Klemp, J. B.: Dynamics of tornadic thunderstorms, *Annu. Rev. Fluid Mech.*, 19, 369–402, 1987.

Marcinoniene, I.: Tornadoes in Lithuania in the period of 1950–2002 including analysis of the strongest tornado of 29 May 1981, *Atmos. Res.*, 67–68, 475–484, 2003.

25 Markowski, P. M., Rasmussen, E. N., and Straka, J. M.: The occurrence of tornadoes in supercells interacting with boundaries during VORTEX-95, *Weather Forecast.*, 13, 852–859, 1998.

Matsangouras, J. T. and Nastos, P. T.: The 27 July 2002 tornado event in Athens, Greece, *Adv. Sci. Res.*, 4, 9–13, doi:10.5194/asr-4-9-2010, 2010.

30 Matsangouras, I. T., Nastos, P. T., and Nikolakis, D.: Study of meteorological conditions related to the tornado activity on 25-3-2009 over NW Peloponnesus, Greece, in: Proc. 10th International Conference on Meteorology, Climatology and Atmospheric Physics (COMECAP2010), 25–38 May 2010, Patras, Greece, 417–425, 2010 (in Greek).



## Analysis of synoptic conditions for tornadic days

P. T. Nastos and  
I. T. Matsangouras

Title Page	
Abstract	Introduction
Conclusions	References
Tables	Figures
◀	▶
◀	▶
Back	Close
Full Screen / Esc	
Printer-friendly Version	
Interactive Discussion	

Matsangouras, I. T., Nastos, P. T., and Sioutas, M. V.: 300 Years Historical Records of Tornadoes, Waterspouts and Funnel Clouds over Greece, 6th European Conference on Severe Storms (ECSS 2011), 3–7 October 2011, Palma de Mallorca, Balearic Islands, Spain, ECSS2011-215, 2011a.

5 Matsangouras, I. T., Nastos, P. T., and Pytharoulis, I.: Synoptic-mesoscale analysis and numerical modeling of a tornado event on 12 February 2010 in northern Greece, *Adv. Sci. Res.*, 6, 187–194, doi:10.5194/asr-6-187-2011, 2011b.

Matsangouras, I. T., Nastos, P. T., and Pytharoulis, I.: Numerical investigation of the role of topography in tornado events in Greece, in: *Advances in Meteorology, Climatology and Atmospheric Physics*, edited by: Helmis, C. G. and Nastos, P. T., Springer, Berlin, Heidelberg, doi:10.1007/978-3-642-29172-2\_30, 209–215, 2012.

10 Matsangouras, I. T., Nastos, P. T., Bluestein, H. B., and Sioutas, M. V.: A climatology of tornadic activity over Greece based on historical records, *Int. J. Climatol.*, in press, doi:10.1002/joc.3857, 2014.

15 Meaden, G. T.: Tornadoes in Britain: their intensities and distribution in space and time, *J. Meteorol.*, 1, 242–251, 1976.

Miller, R. C.: Notes on analysis and severe-storm forecasting procedures of the Air Force Global Weather Central, AWS Tech. Rep. 200 (rev.), Air Weather Service, Scott AFB, IL, 190 pp., 1972.

20 Nastos, P. T. and Matsangouras, J. T.: Tornado activity in Greece within the 20th century, *Adv. Geosci.*, 26, 49–51, doi:10.5194/adgeo-26-49-2010, 2010.

Nastos, P. T. and Matsangouras, I. T.: Composite mean and anomaly of synoptic conditions for tornadic days over North Ionian Sea (NW Greece), in: *Advances in Meteorology, Climatology and Atmospheric Physics*, edited by: Helmis, C. G. and Nastos, P. T., Springer, Berlin, Heidelberg, doi:10.1007/978-3-642-29172-2\_91, 639–645, 2012.

25 Paul, J. F.: An inventory of tornadoes in France, *Weather*, 54, 217–219, 1999.

Peterson, R. E.: Tornadic Activity in Europe – The Last Half-Century, *Conference on Severe Local Storms*, 63–66, 1982.

Peterson, R. E.: Letzmann and Koschmieder’s “Guidelines for research on funnels, tornadoes, waterspouts and whirlwinds”, *B. Am. Meteorol. Soc.*, 73, 597–611, 1992.

30 Peterson, R. E.: Johannes Peter Letzmann: pioneer tornado researcher, in: *Meteorology in Estonia in Johannes Letzmann’s Times and Today*, edited by: Eelsalu, H. and Tooming, H., Estonian Academy Publishers, 9–43, 1995.



## Analysis of synoptic conditions for tornadic days

P. T. Nastos and  
I. T. Matsangouras

Title Page

Abstract

Introduction

Conclusions

References

Tables

Figures

⏪

⏩

◀

▶

Back

Close

Full Screen / Esc

Printer-friendly Version

Interactive Discussion



- Peterson, R. E.: A historical review of tornadoes in Italy, *J. Wind Eng. Ind. Aerod.*, 74–76, 123–130, 1998.
- Rauhala, J. and Schultz, D. M.: Synoptic climatology of tornadoes in Finland, 5th European Conference on Severe Storms (ECSS 2009), 12–16 October 2009, Landshut, Germany, ECSS2009-55, 2009.
- Rauhala, J., Brooks, E. H., and Schultz, M. D.: Tornado climatology of Finland, *Mon. Weather Rev.*, 140, 1446–1456, 2012.
- Reynolds, D. J.: A revised UK tornado climatology, 1960–1989, *J. Meteorol.*, 24, 290–321, 1999a.
- Reynolds, D. J.: European tornado climatology 1960–1989, *J. Meteorol.*, 24, 376–403, 1999b.
- Rotunno, R.: Numerical simulation of a laboratory vortex, *J. Atmos. Sci.*, 34, 1942–1956, 1977.
- Rotunno, R.: A note on the stability of a cylindrical vortex sheet, *J. Fluid Mech.*, 87, 761–771, 1978.
- Rotunno, R.: A study in tornado-like vortex dynamics, *J. Atmos. Sci.*, 36, 140–155, 1979.
- Rotunno, R.: Vorticity dynamics of a convective swirling boundary layer, *J. Fluid Mech.*, 97, 623–40, 1980.
- Rotunno, R.: An investigation of a three-dimensional asymmetric vortex, *J. Atmos. Sci.*, 41, 283–298, 1984.
- Rotunno, R.: The Fluid Dynamics of Tornadoes, *Annu. Rev. Fluid Mech.*, 45, 59–84, 2013.
- Setvák, M., Šálek, M., and Munzar, J.: Tornadoes within the Czech Republic: from early medieval chronicles to the “internet society”, *Atmos. Res.*, 67–68, 589–605, 2003.
- Sioutas, M. V.: Tornadoes and waterspouts in Greece, *Atmos. Res.*, 67–68, 645–656, 2003.
- Sioutas, M. V.: A tornado and waterspout climatology for Greece, *Atmos. Res.*, 100, 344–356, 2011.
- Sioutas, M. V. and Keul, A. G.: Waterspouts of the Adriatic, Ionian and Aegean Sea and their meteorological environment, *Atmos. Res.*, 83, 542–557, 2007.
- Smart, D. J. and Browning, K. A.: Morphology and evolution of cold-frontal mesocyclones, *Q. J. Roy. Meteor. Soc.*, 639, 381–393, 2009.
- Tarand, A.: How often do tornadoes occur in Estonia?, in: *Meteorology in Estonia in Johannes Letzmann’s Times and Today*, edited by: Eelsalu, H. and Tooming, H., Estonian Academy Publishers, 132–138, 1995.

Tooming, H. K. and Peterson, R. E.: Vigorous tornadoes and waterspouts during the last 35 years in Estonia, in: *Meteorology in Estonia in Johannes Letzmann's Times and Today*, Eelsalu, H. and Tooming, H., Estonian Academy Publishers, 168–179, 1995.

5 Tyrrell, J.: Tornadoes in Ireland: an historical and empirical approach, *Atmos. Res.*, 56, 281–290, 2001.

Wegener, A.: *Wind- und Wasserhosen in Europa*, Vieweg, Braunschweig, 301 pp., 1917.

Wilson, T. and Rotunno, R.: Numerical simulation of a laminar end-wall vortex and boundary layer, *Phys. Fluids*, 29, 3993–4005, 1986.

## Analysis of synoptic conditions for tornadic days

P. T. Nastos and  
I. T. Matsangouras

Title Page

Abstract

Introduction

Conclusions

References

Tables

Figures



Back

Close

Full Screen / Esc

Printer-friendly Version

Interactive Discussion



## Analysis of synoptic conditions for tornadic days

P. T. Nastos and  
I. T. Matsangouras

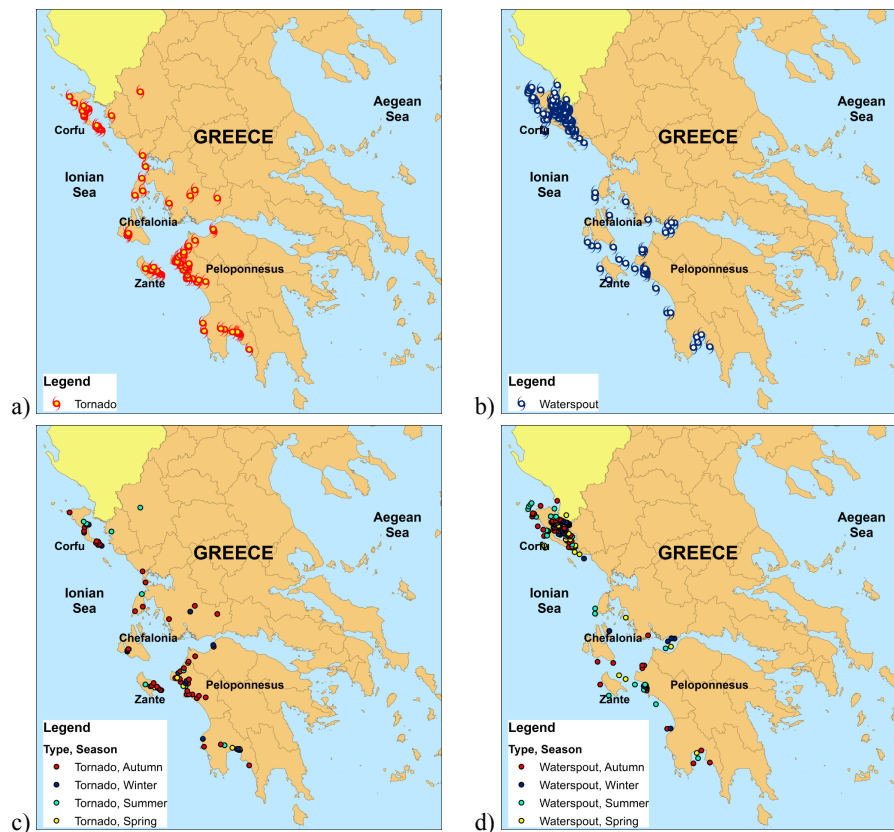


**Fig. 1.** Annual spatial distribution of tornadoes (a) and waterspouts (b), along with the seasonal spatial distribution of tornadoes (c) and waterspouts (d) over Greece for the period 12 August 1953–31 December 2012.

[Title Page](#)
[Abstract](#)
[Introduction](#)
[Conclusions](#)
[References](#)
[Tables](#)
[Figures](#)
[Back](#)
[Close](#)
[Full Screen / Esc](#)
[Printer-friendly Version](#)
[Interactive Discussion](#)

## Analysis of synoptic conditions for tornadic days

P. T. Nastos and  
I. T. Matsangouras

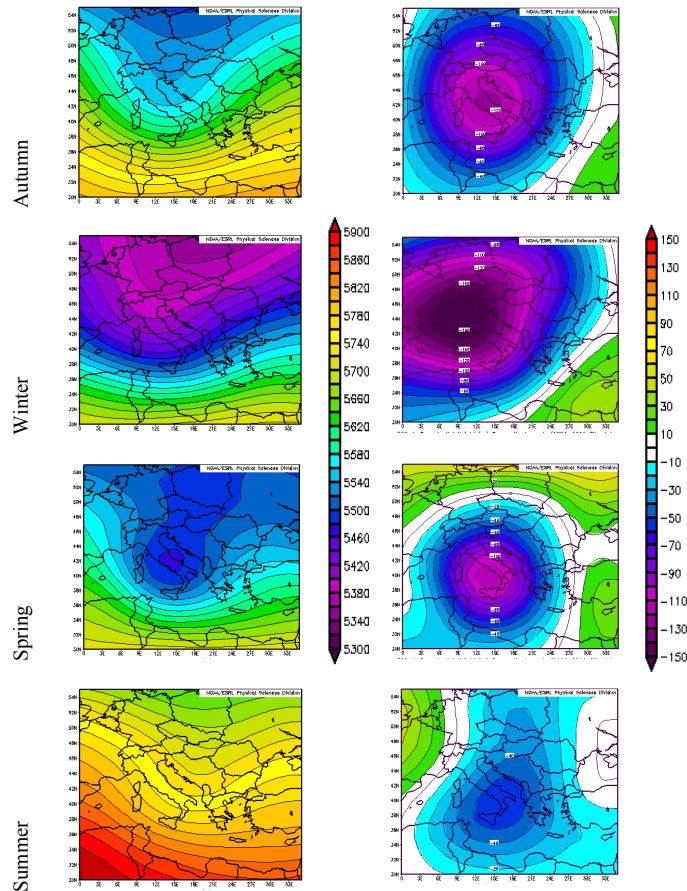


**Fig. 2.** Seasonal daily composite means (left column) and anomalies (right column) of geopotential heights at 500 hPa isobaric level for tornado days over Greece for the period 12 August 1953–31 December 2012.

[Title Page](#)
[Abstract](#)
[Introduction](#)
[Conclusions](#)
[References](#)
[Tables](#)
[Figures](#)
[⏪](#)
[⏩](#)
[◀](#)
[▶](#)
[Back](#)
[Close](#)
[Full Screen / Esc](#)
[Printer-friendly Version](#)
[Interactive Discussion](#)

## Analysis of synoptic conditions for tornadic days

P. T. Nastos and  
I. T. Matsangouras

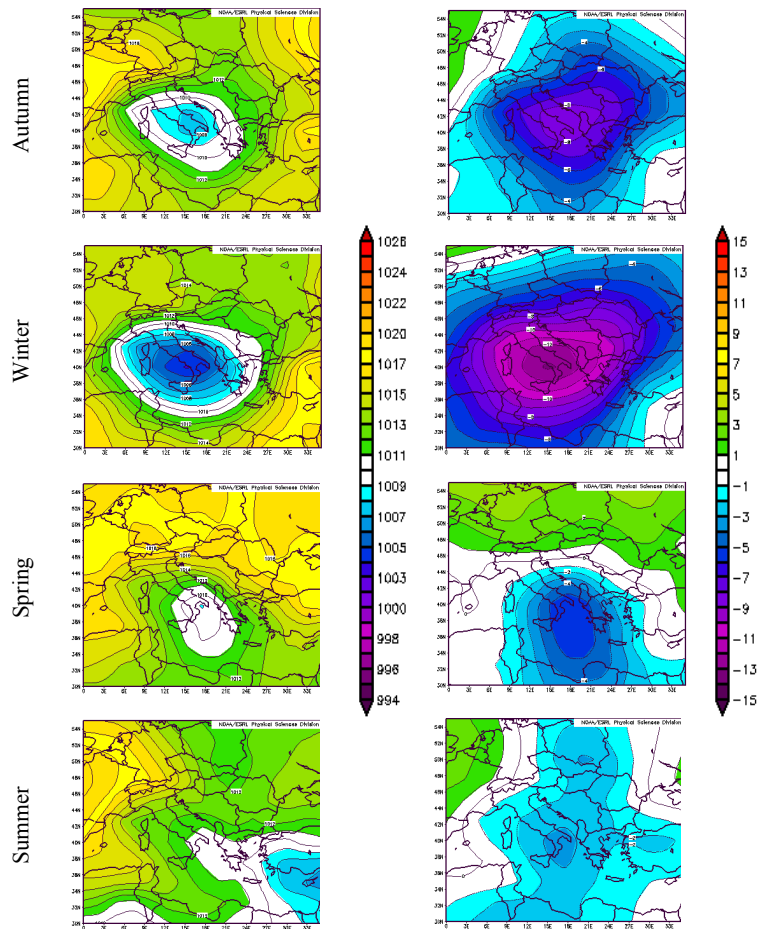


**Fig. 3.** Seasonal daily composite means (left column) and anomalies (right column) of sea level pressure for tornado days over Greece for the period 12 August 1953–31 December 2012.

## Analysis of synoptic conditions for tornadic days

P. T. Nastos and  
I. T. Matsangouras

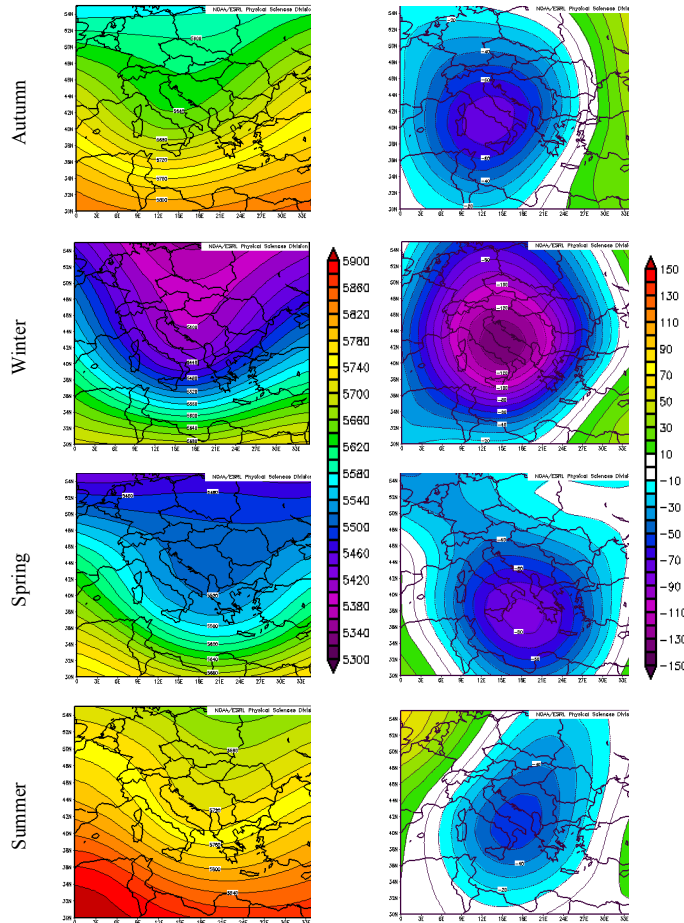


**Fig. 4.** Seasonal daily composite means (left column) and anomalies (right column) of geopotential heights at 500 hPa isobaric level for waterspout days over Greece for the period 12 August 1953–31 December 2012.

Title Page

Abstract	Introduction
Conclusions	References
Tables	Figures

⏪      ⏩  
◀      ▶  
Back      Close

Full Screen / Esc

Printer-friendly Version

Interactive Discussion



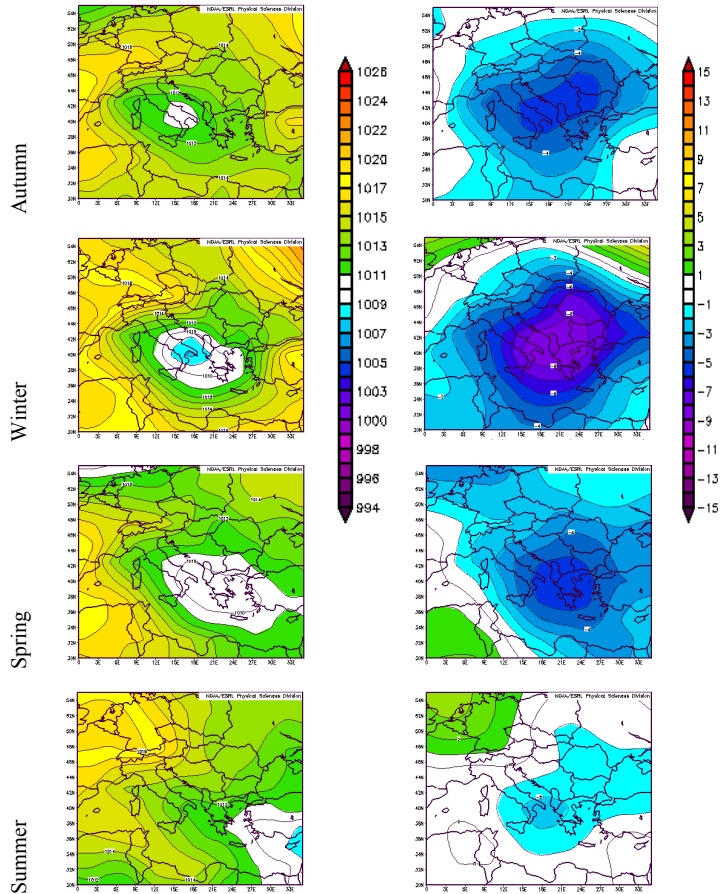


**Fig. 5.** Seasonal daily composite means (left column) and anomalies (right column) of sea level pressure for waterspout days over Greece for the period 12 August 1953–31 December 2012.

**Analysis of synoptic conditions for tornadic days**

P. T. Nastos and  
I. T. Matsangouras

Title Page

Abstract

Introduction

Conclusions

References

Tables

Figures

⏪

⏩

◀

▶

Back

Close

Full Screen / Esc

Printer-friendly Version

Interactive Discussion



## Analysis of synoptic conditions for tornadic days

P. T. Nastos and  
I. T. Matsangouras

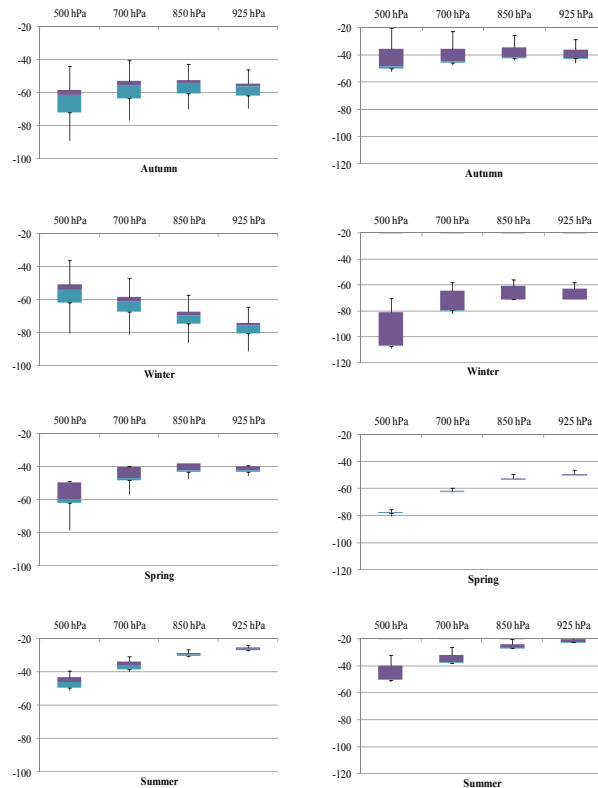


**Fig. 6.** Box and whiskers plots of seasonal daily anomalies of the geopotential heights (m) at isobaric levels of 500 hPa, 700 hPa, 850 hPa and 925 hPa, for tornadoes (left column) and waterspouts (right column), calculated at the location of each event in west Greece, from 12 August 1953 to 31 December 2012. The horizontal line in the box represents the median, the box represents the 25th and 75th percentile and the whiskers refer to maximum and minimum daily anomalies.

[Title Page](#)
[Abstract](#)
[Introduction](#)
[Conclusions](#)
[References](#)
[Tables](#)
[Figures](#)
[⏪](#)
[⏩](#)
[◀](#)
[▶](#)
[Back](#)
[Close](#)
[Full Screen / Esc](#)
[Printer-friendly Version](#)
[Interactive Discussion](#)

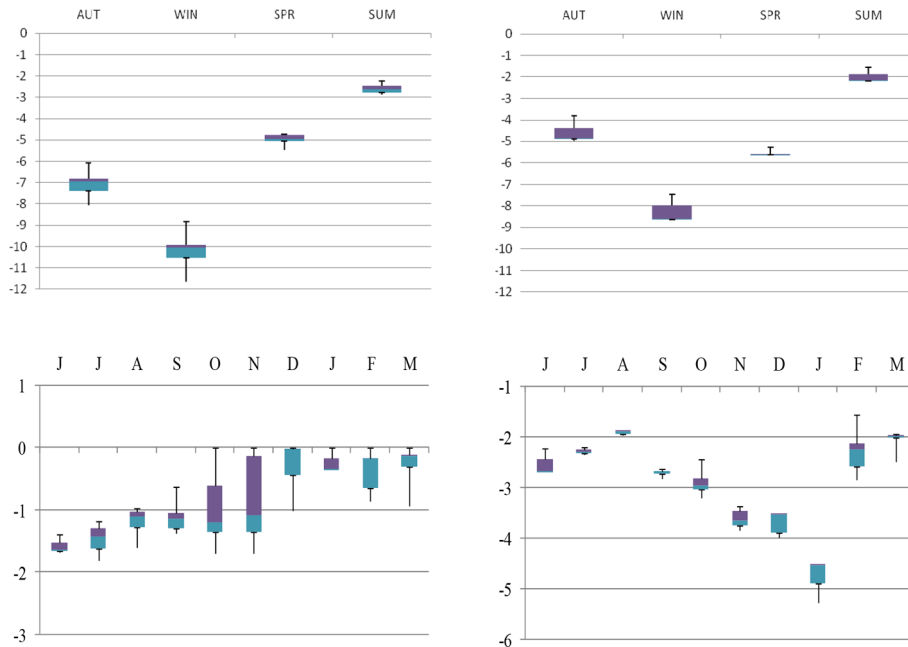


**Fig. 7.** Box and whiskers plots of seasonal daily anomalies of the sea level pressure (hPa) for tornadoes (upper left graph) and waterspouts (upper right graph) calculated at the location of each event in west Greece, from 12 August 1953 to 31 December 2012. Lower graphs depict Box and whiskers plots of monthly (June to March) daily means (lower left graph) and anomalies (lower right) of Lifted Index (LI), based on NCER-NCAR reanalysis datasets during tornado days over west Greece for the period 12 August 1953–31 December 2012. The horizontal line in the box represents the median, the box represents the 25th and 75th percentile and the whiskers refer to maximum and minimum daily anomalies.

**Analysis of synoptic conditions for tornadic days**

P. T. Nastos and  
I. T. Matsangouras

Title Page	
Abstract	Introduction
Conclusions	References
Tables	Figures
◀	▶
◀	▶
Back	Close
Full Screen / Esc	
Printer-friendly Version	
Interactive Discussion	



**Analysis of synoptic conditions for tornadic days**P. T. Nastos and  
I. T. Matsangouras

**Fig. 8.** Cold front activity associated to pre-frontal tornado occurrence during autumn season from 2006 to 2012. Flag symbols correspond to impacts on crops (green flag), structures (orange flag), crops + structures (red flag) during tornado days over west Greece the period 12 August 1953–31 December 2012.